

CHEMICALLY ACTIVATED KAOLINITES AFTER DE-INTERCALATION OF FORMAMIDE

MARTA VALÁŠKOVÁ, GRAŽYNA SIMHA MARTYNKOVÁ, VLASTIMIL MATĚJKO, GABRIELA KRATOŠOVÁ

*Institute of Materials Chemistry, VŠB-Technical University of Ostrava,
17. listopadu 15/2172; 708 33 Ostrava-Poruba, Czech Republic*

E-mail: marta.valaskova@vsb.cz

Submitted March 2, 2006; accepted September 28, 2006

Keywords: Powders-chemical preparation; De-intercalation; X-ray diffraction; Kaolinite, Structural application.

Five well and poor ordered kaolinites were studied to explore structural changes of kaolinite/formamide intercalates and de-intercalates. These materials were evaluated using the X-ray powder diffraction (XRPD) supplement with scanning electron microscope (SEM), measurement of specific surface area (SSA) and particle size distribution (PSD). The XRPD of de-intercalated kaolinites exhibit: (1) diffractions of 7 Å kaolinite, some remaining 10 Å kaolinite/formamide complex and an additional 8.4 Å phase, (2) lower one-layer thickness of de-intercalated 7 Å kaolinite than before formamide treatment, (3) changes in the (02, 11) diffraction band indicating structural disorder in the a, b plane. The chemical activation of kaolinites using formamide creates kaolinites with smaller and more homogenous particles and higher SSA than were observed in the original ones.

INTRODUCTION

The industrial delamination of kaolinite promote fractures of flat plates along the 001 basal plane, degradation of crystal structure and separation of kaolinite particles into thin platelets. The thickness of kaolinite particles affects coating paper properties and ceramics properties [1-3]. In the past few years, applications related to the sorption properties of kaolinite have been developed. Unfortunately, the sorption capacity of natural kaolinite is limited because of a small specific surface area (SSA). Therefore the mechanical grinding is applied to improve physicochemical activity of kaolinite [4-8]. Aglietti et al. [5] found out that ground kaolinite appears to be more active for next thermal transformation. Kristóf et al. [8] stated that 1h of kaolinite amorphization is necessary for formation of mullite-type crystals at reduced temperature of 1000°C. Suraj et al. [9] obtained after grinding for 10 min the separated platelets of micronized kaolinite with the SSA increasing from 15 to 32 m² g⁻¹. However, an extension grinding causes agglomeration of platelets into small balls with an amorphous surface layers and a reduction of the SSA [6, 7, 9-11]. Micronized kaolinite particles were tested for sorption of heavy metals [9] and water vapour [4]. The physicochemical activity of kaolinites with different degree of structural order studied Gonzalez Garcia et al. [7] and Sánchez-Soto et al. [10]. The SSA in well-ordered kaolinites increased from 15.0 to 38.7 m²/g after grinding time of 36 h [7] and from 10.2 m²/g to 18.3 m²/g after 15 min of grinding [10].

The SSA of poor-ordered kaolinite was larger than that of well-ordered kaolinite and decreased noticeable on grinding for 8 h [7]. Sánchez-Soto et al. observed also that SSA in poorly ordered kaolinite increases from 19.8 m²/g to 38.67 m²/g and 50.3 m²/g on grinding 15 min and 30 min, respectively. The grinding prolongation above 30 min agglomerated particles and reduced the SSA [10].

The reactivity of the kaolinite surface can be tested through its modification using intercalation with organic molecules. Most often used molecules are formamide, urea, potassium acetate, dimethylsulfoxide or hydrazine [11-17]. Frost et al. studied changes of the surface of kaolinite with combination of dry grinding of kaolinite followed by intercalation with formamide. Using X-ray diffraction authors observed that intensity of the first basal diffraction of kaolinite ($d_{001} = 7.1 \text{ \AA}$) with grinding time decreases as well as intensity of kaolinite/formamide complex ($d_{001} = 10.2 \text{ \AA}$). Kaolinite upon 3 h of grinding is not able to intercalate with formamide [18]. Frost et al. analyzed a mechanochemically activated kaolinite intercalated with formamide, which was aged for up to 1 year. They stated that the mechanochemically activated kaolinite results in de-intercalation of the formamide and de-intercalated kaolinite returns to its original d -spacing [19]. Horváth et al. [20] observed the formation of highly active surface sites at the kaolinite after de-intercalation of formamide. Their selective sorption properties and formation of CO₂ complexes decreased with the grinding time.

These works present a view of preparation and mechanochemical techniques used for activation of kaolinite material. On this account we decided to attend only the chemically activated kaolinites with different degree of structural order using intercalation with formamide. Activated kaolinites are evaluated from the kaolinite/formamide de-intercalates and compared with their original samples.

MATERIAL AND METHODS

Material

For experiments we used kaolinites (*Ka*) from the collection of Chmielová and Weiss [21] (Table 1). The original samples were passed through a 0.045 mm sieve and subjected to timed sedimentation to obtain fraction less than 2 µm. Complexes (*Ka/FA*) with formamide (FA), H–C(=O)–NH₂, (Fluka), were prepared from kaolinite sample mixed with FA in mass ratio 1:1. Afterwards, samples were placed in closed flasks in order to realize penetration formamide into kaolinite interlayer. The kaolinite/formamide samples were examined using X-ray diffraction in two steps: (1) after 3 days when the samples still had a wax-like appearance (intercalates *Ka/FA-3*), and (2) after 40 days of evaporation of formamide (de-intercalates *Ka/FA-40*), when on the X-ray patterns basal diffractions of kaolinite regenerate and diffractions of *Ka/FA* complex disappear. Original kaolinites Jimlíkov (*Jim*) and Sedlec (*Sed*) with different structural order and their de-intercalates *Jim/FA-40* and *Sed/FA-40* were selected for particle size distribution and specific surface area measurements.

Methods

The X-ray powder diffraction (XRPD) patterns were recorded at 30 kV and 20 mA, exposure time 2000 seconds with CuK α_1 radiation in the reflection mode (INEL CPS 120 equipped with a curved position-sensitive detector and a germanium monochromator). Samples were positioned in a flat rotation holder. The *d* measurements are accompanied by their standard deviation given in units of the last significant digit. The peak

Table 1. Kaolinite samples and symbols used in text, Hinckley index (HI) and particle size parameters.

Kaolinites (<i>Ka</i>)	Symbol	HI	PSD - max ^a (µm)
1. Božičany	<i>Boz</i>	0.30	2.7
2. Únanov	<i>Un</i>	0.48	2.6
3. Sedlec	<i>Sed</i>	0.63	2.2
4. Jimlíkov	<i>Jim</i>	1.06	1.5
5. Horní Bříza	<i>Bri</i>	1.47	2.8

^a Particle size diameter corresponding to the maximum of particle size distribution

intensities and angle positions, particularly of overlapping diffractions, were evaluated using the computer program DIFPATAN [22]. Specific surface area (SSA) was determined at liquid-nitrogen temperature by means of Sorptomatic 1990, employing the BET methodology. Nitrogen gas was used as an adsorbate. Kaolinite particles were observed on a scanning electron microscope (SEM), Philips XL 30. Samples were coated with gold/palladium film and the SEM-images were obtained using a secondary electron detector. Particle size distribution (PSD) measurement was performed on Fritsch Particle Sizer Analysette 22.

RESULTS AND DISCUSSION

Kaolinite (*Ka*) samples

The Hinckley index, HI, [23], calculated for five kaolinite samples ranges from 0.30 to the 1.47 (Table 1). Kaolinites *Boz*, *Un* and *Sed* with HI < 0.8 have a low degree of structural order, kaolinite *Jim* with HI = 1.06 and kaolinite *Bri* with HI = 1.47 have medium and high degree of structural order, respectively [21]. The measured X-ray data previously evaluated [21] using Expert System [24] with the aim to characterize defects in kaolinite structures allow to classify kaolinites *Boz*, *Un* and *Sed* as single phases with the average number of 33 kaolinite layers in the coherent diffraction domains and translation defects between adjacent layers; kaolinites *Jim* and *Bri* are mixtures of 49.8 % and of 81.6 % of low-defect phase, respectively, and remaining high-defect phase. No impurities in the prepared *Ka* < 2 µm fractions were detected, except the *Bri*, where ~ 4 wt. % of mica admixture was determined. The average values of the first and second basal spacings calculated for the *Ka* samples are *d*₀₀₁ = 7.113(34) Å and *d*₀₀₂ = 3.554(17) Å.

Ka/FA-3 intercalates

The XRPD patterns of *Ka/FA-3* intercalates appear in Figure 1a. The kaolinite/formamide intercalate complexes have the first basal diffraction (001_c) at ~ 10 Å, which indicates that the kaolinite structure has expanded along its c-axis. There is a residual 001 diffraction at ~ 7 Å suggesting that some portion of kaolinite is not affected by the treatment, but its basal spacing and intensity differs from the original ones (Table 2). The average basal spacing of non-affected *Ka* are slightly lower than at original samples: *d*₀₀₁ = 7.055(57) Å and *d*₀₀₂ = 3.530(30) Å. The *Ka/FA-3* complexes show strong first (001_c) and third (003_c) basal diffractions with average values of *d*_{001c} = 10.022(111) Å and *d*_{003c} = 3.345(40) Å. The degree of contraction of the basal spacing was calculated using the intercalation ratio (IR), in accord with Wiewióra & Brindley [25]. Integrated

intensities I_7 of the first basal diffraction of kaolinite ($d_{001} \sim 7 \text{ \AA}$) and I_{10} of the Ka/FA complex ($d_{001c} \sim 10 \text{ \AA}$) were input in the equation IR = $I_{10}/(I_{10} + I_7)$, (Table 2). Accordingly, the IR is zero for untreated kaolinite and unity for a completely intercalated one. Kaolinite *Bri* with high degree of structural order shows a high intercalation ratio (IR = 0.84). Kaolinites *Jim* with a medium and *Boz, Un, Sed* with a low degree of structural order yield a similar intercalation ratio of IR = 0.46(4).

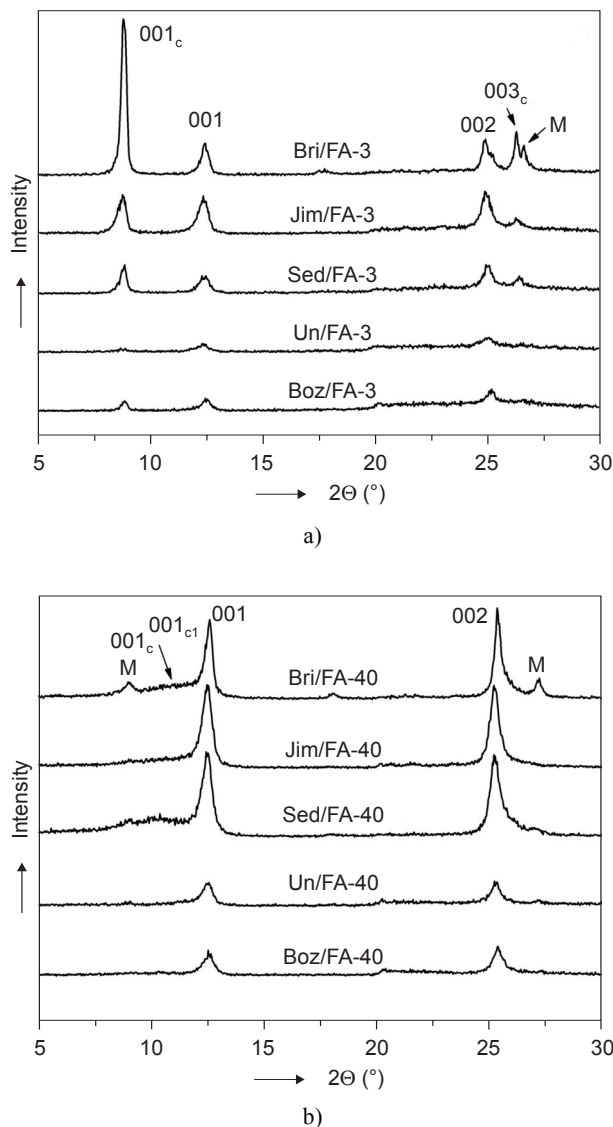


Figure 1. The XRPD patterns (fragments from 5-30° with the basal diffractions) of the kaolinite/formamide intercalate complexes measured after a) 3 days (Ka/FA-3) and b) after 40 days (Ka/FA-40). The basal diffractions: 001, 002 = first and second of kaolinite; 001_c, 003_c = the first and third of kaolinite/formamide intercalate complex; 001_{c1} = the first of kaolinite + kaolinite/formamide or kaolinite/water domains. M = the first and third basal diffractions of mica.

Ka/FA-40 de-intercalates

In all samples, de-intercalation by evaporation of FA results in a recovery of the 7 Å-kaolinite structure. The penetration of FA into kaolinite interlayer must have caused change of layered structure. A comparison of XRPD patterns of the Ka/FA-3 intercalates (Figure 1a) and Ka/FA-40 de-intercalates (Figure 1b) shows that all samples are partially de-intercalated because besides the intensive kaolinite 001 and 002 basal diffractions with an average $d_{001} = 7.051(15) \text{ \AA}$ and $d_{002} = 3.506(10) \text{ \AA}$ there are: a) residual basal diffractions 001_c and 003_c of the Ka/FA complex with an average basal spacing values $d_{001c} = 9.784(43) \text{ \AA}$ and $d_{003c} = 3.281(15) \text{ \AA}$, and b) additional low-intensity 001_{c1} diffraction with an average value $d_{001c1} = 8.369(126) \text{ \AA}$.

Table 2. X-ray diffraction results of original kaolinite samples, kaolinite/formamide intercalates and kaolinite/formamide de-intercalates.

Sample	d_{001c} (Å)	d_{001c1} (Å)	d_{001} (Å)	d_{002} (Å)	d_{003c} (Å)	IR
1. <i>Boz</i>				7.145	3.558	
Boz/FA-3	9.847		6.962	3.478	3.276	0.45
Boz/FA-40	9.729	8.515	7.033	3.495	3.298	0.09
2. <i>Un</i>			7.080	3.541		
Un/FA-3	10.068	8.267	7.096	3.542	3.346	0.40
Un/FA-40	9.849		7.062	3.510	3.267	0.11
3. <i>Sed</i>			7.132	3.565		
Sed/FA-3	9.990		7.104	3.543	3.356	0.50
Sed/FA-40	9.771	8.488	7.069	3.511	3.290	0.13
4. <i>Jim</i>			7.073	3.532		
Jim/FA-3	10.067		7.062	3.533	3.372	0.49
Jim/FA-40	9.785	8.240	7.042	3.516	-	0.10
5. <i>Bri</i>			7.136	3.573		
Bri/FA-3	10.137		7.052	3.555	3.375	0.84
Bri/FA-40	9.784	8.334	7.051	3.496	3.269	0.20

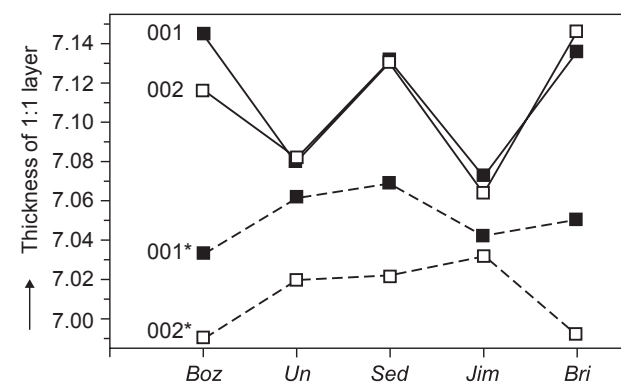


Figure 2. The thickness of the kaolinite layer by the d (Å) of the first and second basal diffractions (001, 002) of the original kaolinite samples in comparison with the (001*, 002*) of chemically activated kaolinites from kaolinite/formamide de-intercalates.

The changes in the basal diffraction region are observed at all Ka/FA-40 de-intercalates. The thickness of one 7 Å-layer of the original and partially de-intercalated kaolinites is different (Table 2). If we express the thickness of one kaolinite layer by the d of the first and second basal diffractions (Figure 2) we can see that it is lower for all kaolinites after formamide de-intercalation than it was in the original material. In addition to this, the d_{002} appears systematically lower than one-half of d_{001} . A new-formed ~9.8 Å and ~8.4 Å phases, separated from 7 Å phase, may correspond to a one-layer kaolinite/formamide complex or to the kaolinite domains

with formamide or water. Examples of such change in the interlayer basal spacing are performed on the XRPD patterns of Jim, Jim/FA-3 intercalate and Jim/FA-40 de-intercalate in Figure 3. Intensive 001 and 002 basal diffractions of Jim (Figure 3 a) are compared with non-intercalated ones and also with the basal diffractions 001_c and 003_c of Jim/FA complex in Figure 3b. The XRPD pattern of Jim/FA-40 in Figure 3c shows: (1) kaolinite 001 and 003 diffractions, (2) residuum of 001_c diffraction and (3) low-intensity diffraction 001_{cl} of a newly appearing 8.24 Å phase.

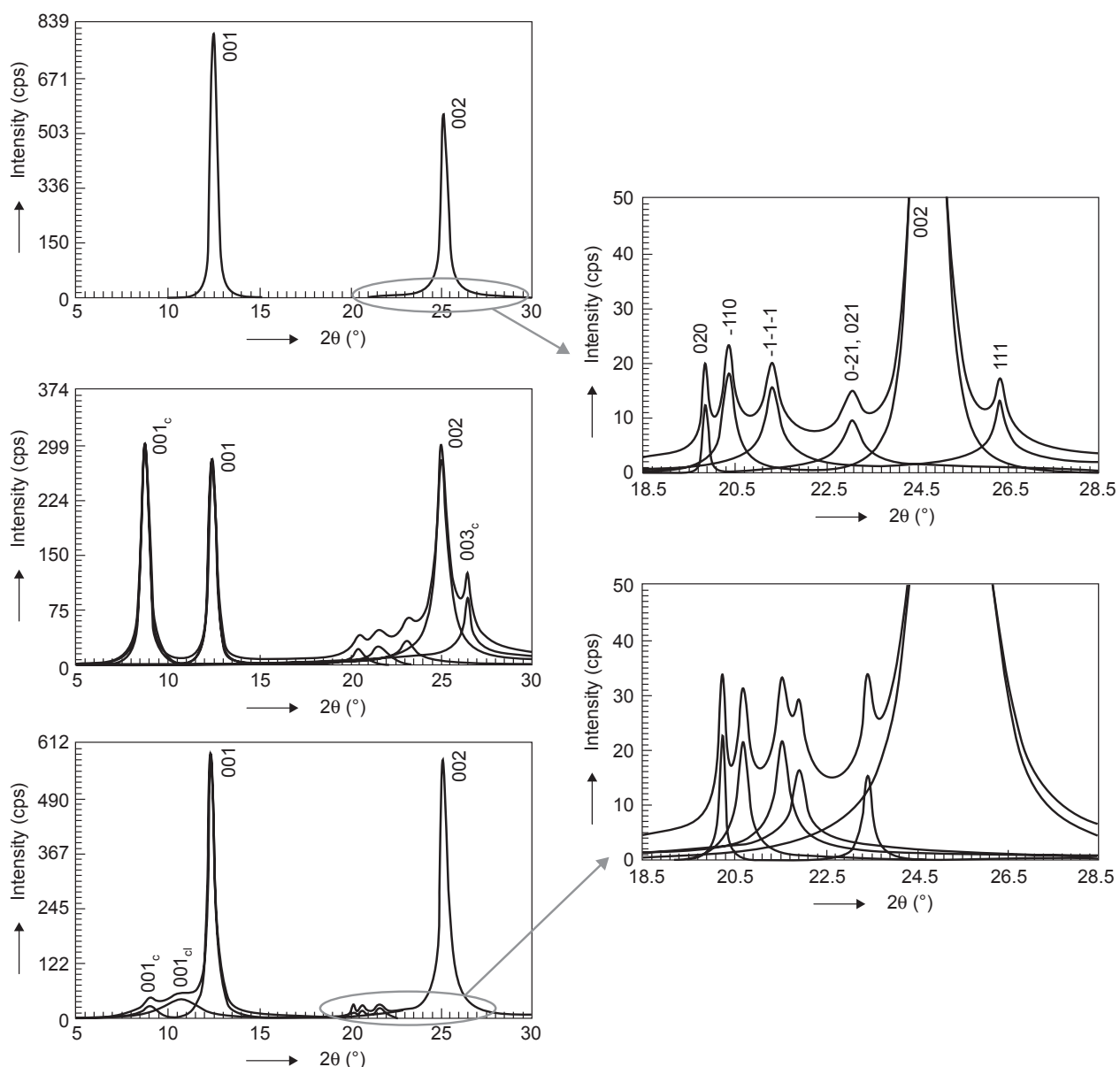


Figure 3. The XRPD patterns (fragment from 5-30 °2θ) after procedure DIFPATAN [22]: a) kaolinite Jim, b) Jim/FA-3 and c) Jim/FA-40. The basal diffractions: 001, 002 = first and second of kaolinite; 001_c, 003_c = first and third of kaolinite/formamide intercalate complex; 001_{cl} = the first of kaolinite + kaolinite/formamide or kaolinite/water domains. The (02, 11) diffraction band of the original kaolinite Jim is compared with the band of chemically activated kaolinite Jim/FA-40 from kaolinite/formamide de-intercalates on the right side.

The intercalation not only increases the basal interlayer spacing but also changes the stacking sequence so the adjacent layers are shifted along *a*, *b* axes. A stacking fault between layers of kaolinite with translation defects affects diffractions of the $02(l)$, $11(l)$ type with $l = 0, 1, 2$ in the $(02, 11)$ diffraction band [26, 27]. The changes observed on the $(02, 11)$ diffraction band at studied Ka/FA-40 de-intercalates are performed on the right side of Figure 3. The doubled diffractions and the angular shifts at Jim/FA-40 indicate enhancement of structural disorder probably due to the simultaneous presence of both well and low ordered kaolinite and/or due to the translation defects.

From the particle size distribution (PSD) measurement the percentage fraction of particles smaller than 2 μm is 78 vol. % for *Jim* and 72 vol. % for *Sed*. Particle size diameter corresponding to the maximum of particle distribution is 1.5 μm and 2.1 μm for *Jim* and *Sed*, respectively. The SEM micrographs give information

about the evolution of particles after formamide de-intercalation (Figures 4). The original samples *Jim* and *Sed* have quite heterogeneous particle size distributions and consist of submicron particles and stacks of flakes (Figures 4a, 4b). Jim/FA-40 has platy particles more homogenous in particle size and slightly smaller (Figure 4c) than original *Jim*. The Sed/FA-40 (Figure 4d) indicates resulting plates similar to the original *Sed*. The particle size distributions obtained after de-intercalation show small increase of particles smaller than 2 μm (to the 79 vol. % for Jim/FA-40 and only to the 74 vol. % for Sed/FA-40). Particle size diameter corresponding to the maximal frequency of particles after formamide de-intercalation indicates that the resulting platelets are similar to the original ones (1.43 μm for Jim/FA-40 and 2.1 μm for Sed/FA-40).

Chemically activated kaolinites using intercalation with formamide show increase in the specific surface area. If compare natural kaolinites with distinct degree

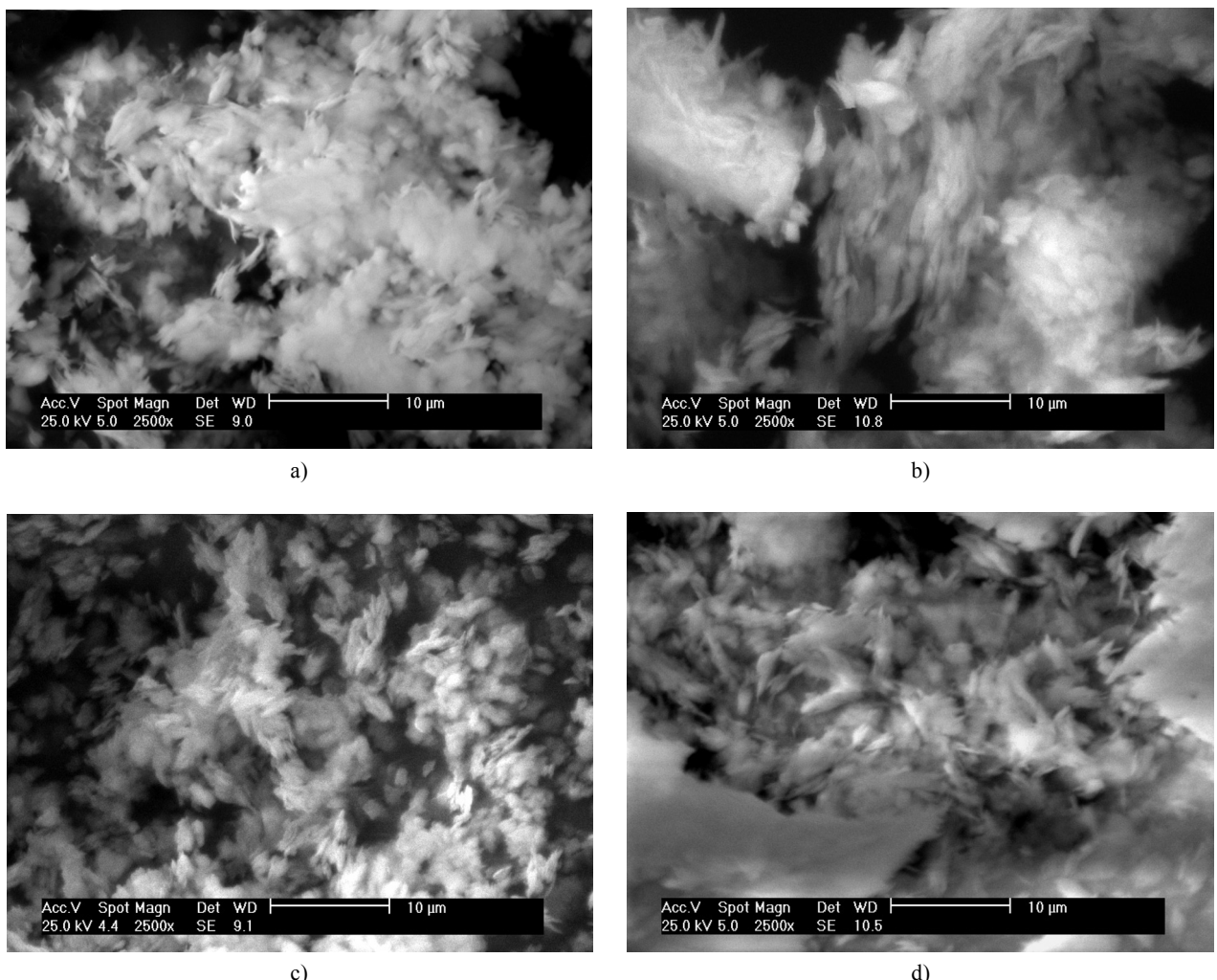


Figure 4. The SEM micrographs of the original kaolinite samples *Jim* (a), *Sed* (b) and of chemically activated kaolinites from kaolinite/formamide de-intercalates *Jim/FA-40* (c) and *Sed/FA-40* (d).

of structural order we can see that specific surface area measured at poor-ordered *Sed* ($\text{SSA} = 17.8 \text{ m}^2/\text{g}$) is slightly larger than that of medium-ordered *Jim* ($\text{SSA} = 12.3 \text{ m}^2/\text{g}$). The identical properties observed for kaolinites with different structural ordering Gonzalez Garcia et al. [6]. Chemically activated poor-ordered *Sed/FA-40* shows slightly lower increase SSA (from $17.8 \text{ m}^2/\text{g}$ to $22.7 \text{ m}^2/\text{g}$) than medium-ordered *Jim/FA-40* (from $12.3 \text{ m}^2/\text{g}$ to $21.0 \text{ m}^2/\text{g}$). The SSA discrepancy may be explained by distribution and anisotropy of particles rather than by the structural ordering.

CONCLUSIONS

Chemically activated kaolinites with formamide after 40 days result in partially de-intercalated 7 \AA kaolinites with one-layer thickness lower in comparison with the original kaolinites and additional phases with a spacing of $\sim 9.8 \text{ \AA}$ and $\sim 8.4 \text{ \AA}$. The kaolinite after de-intercalation of formamide becomes a) more disordered due to the redistribution of layers with different content of defect domains, which may be due to a one-layer kaolinite/formamide complex or to other layers or parts of layers with formamide or water, b) higher homogeneity of particle size in comparison with original samples, c) larger in surface area.

Acknowledgement

Financial support of the Ministry of Education of the Czech Republic (project MSM 6198910016) and the Czech Grant Agency (project GA ČR No. 205/05/2548) are gratefully acknowledged.

References

- Prasad M., Reid K., Murray H.: *Appl.Clay Sci.* **6**, 87 (1991).
- Bundy W., Ishley J.: *Appl.Clay Sci.* **5**, 397 (1991).
- Murray H., Bundy W., Harvey C.: *The Clay Minerals Society*, Boulder, Colorado, 1993, 341 pp.
- Hlavay J., Jonas K., Elek S., Inczedy J.: *Clays Clay Miner.* **25**, 451 (1977).
- Aglietti E.F., Porto López J.M., Pereira E.: *Int.J.Miner. Process* **16**, 125 (1986a).
- Aglietti E.F., Porto López J.M., Pereira E.: *Int.J.Miner. Process* **16**, 135 (1986b).
- Gonzalez Garcia F., Ruiz Abrio M.T., Gonzalez Rodriguez M.: *Clay Miner.* **26**, 549 (1991).
- Kristóf É., Juhász A.Z., Vassányi I.: *Clays Clay Miner.* **41**, 608 (1993).
- Suraj G., Iyer C.S.P., Rugmini S., Lalithambika, M.: *Appl. Clay Sci.* **12**, 111 (1997).
- Sánchez-Soto P.J., Jiménez de Haro M.C., Pérez-Maqueda L.A., Varona I., Pérez-Rodríguez J.L.: *J.Am.Ceram.Soc.* **83**, 1649 (2000).
- Frost R.L., Makó E., Kristóf J., Horváth E., Kloprogge J.T.: *J.Colloid Interface Sci.* **239**, 458 (2001).
- Lagaly G.: *Philosophical Transactions of the Royal Society of London. A. Mathem.Phys.Sci.* **311**, 315 (1984).
- Kristóf J., Frost R.L., Kloprogge J.T., Horváth E., Gábor M.: *J.Therm.Anal.Calorim.* **56**, 885 (1999).
- Tsumenatsu K., Tateyama, H., Nishimura S., Jinnai K.: *J.Ceram.Soc.Jpn.* **100**, 178 (1992).
- Maxwell C., Malla P.: *J.Am.Ceram.Soc.Bull.* **78**, 57 (1999).
- Valášková M., Rieder M., Matějka V., Čapková P., Slíva A.: *Appl.Clay Sci.* **35**, 108 (2007).
- Franco F., Ruiz Cruz, M.D.: *Clay Miner.* **39**, 193 (2004).
- Frost R.L., Horváth E., Makó É., Kristóf J., Cseh T.: *J. Colloid Interface Sci.* **236**, 386 (2003).
- Frost R.L., Horváth E., Makó É., Kristóf J., Rédey A.: *Termochim.Acta* **408**, 103 (2003).
- Horváth E., Kristóf J., Frost R.L., Jakab E., Makó E., Vágvölgyi V.: *J. Colloid Interface Sci.* **289**, 132 (2005).
- Chmielová M., Weiss Z.: *Appl.Clay Sci.* **22**, 65 (2002).
- Kužel R. Jr.: *DIFPATAN, Computer Program for X-ray Powder Diffraction Profile Analysis*. Faculty of Mathematics and Physics, Charles University, Prague, 1991.
- Hinckley D.N.: *Clays Clay Miner.* **11**, 229 (1963).
- Plançon A., Zacharie C.: *Clay Miner.* **25**, 249 (1990).
- Wiewióra A., Brindley G.W.: *Proc.Inter.Clay Conf.*, Tokyo **1**, 723 (1969).
- Barrios J., Plançon A., Cruz M.A., Tchoubar C.: *Clays Clay Miner.* **25**, 422 (1977).
- Thompson J.G., Cuff C.: *Clays Clay Miner.* **33**, 490 (1985).

CHEMICKÁ AKTIVACE KAOLINITŮ PO DE-INTERKALACI FORMAMIDU Z KAOLINT/FORMAMIDOVÝCH INTERKALÁTŮ

MARTA VALÁŠKOVÁ, GRAŽYNA SIMHA
MARTYNKOVÁ, VLASTIMIL MATĚJKÁ,
GABRIELA KRATOŠOVÁ

*Centrum nanotechnologií na VŠB-TU Ostrava,
17. listopadu 15/2172; 708 33 Ostrava-Poruba*

Kaolini s různou strukturní neuspořádanosti byly studovány po interkalaci a de-interkalaci formamidu. Připravené kaolinit/formamidové interkaláty a de-interkaláty byly hodnoceny rentgenovou práškovou difrakční (XRPD) analýzou a doplněny hodnotami z měření specifického povrchu (SSA) a údaji o distribuci velikosti částic (PSD). Tvar částic byl hodnocen pod elektronovým mikroskopem (SEM). XRPD analýza de-interkalovaných kaolinitů ukázala, že: (1) vedle 7-A -kaolinitu jsou přítomny zbytek 10-A kaolinit/formamidového interkalátu a nově vzniklá 8.4-A fáze, (2) výška mezivrství u de-interkalovaného 7-A kaolinitu je menší ve srovnání s původním kaolinitem, (3) změny v difrakčním pásu (02, 11) jsou výsledkem strukturní neuspořádanosti v horizontální rovině a, b. Aktivované kaolini po de-interkalaci formamidu mají ve srovnání s původním kaolinitem jednodušší částice a větší specifický povrch.